ADVANCED MATERIALS

www.advmat.de

Novel Multifunctional Properties Induced by Interface Effects in Perovskite Oxide Heterostructures

By *Kui-juan Jin,* Hui-bin Lu,* Kun Zhao, Chen Ge, Meng He,* and *Guo-zhen Yang*

Multilayer structures have emerged as a leading research topic and researchers expect that multilayers may lead to interesting artificial materials with novel properties. In this Research News we show that the introduction of interfaces into perovskite oxides can induce a series of novel properties including an unusual positive magnetoresistance, great enhancement of lateral photovoltage in $La_{0.9}Sr_{0.1}MnO_3/SrNb_{0.01}Ti_{0.99}O_3$, and an electrical modulation of the magnetoresistance in multi-p-n heterostructures of $SrTiO_{3-\delta}/La_{0.9}Sr_{0.1}MnO_3/SrTiO_{3-\delta}/La_{0.9}Sr_{0.1}MnO_3/Si$. This novel positive magnetoresistance is attributed to the creation of a space charge region at the interface where the spin of the carriers is anti-parallel to that of the carriers in the region far from the interface of manganese oxide in the heterostructures.

1. Introduction

Transition metal oxides first made the headlines in 1986 with the Nobel-Prize-winning discovery of high-temperature superconductors. Since then, solid-state physicists keep finding unexpected properties in these materials—including colossal magnetoresistance (CMR), in which small changes in the applied magnetic field cause huge changes in electrical resistance. But the fun really starts when one oxide rubs shoulders with another.[1a] For instance, high mobility[1b] or even superconductivity[1c] can be obtained in the interfacial layer of the heterostructure made by insulating oxides. Researchers are optimistic that they may be able to make combinations of oxides to outperform semiconductor structures.[1a]

Hole-doped manganese oxides with a general formula of $La_{1-x}Sr_xMnO_3$ show remarkable interrelated structural, magnetic, and transport properties. They exhibit a very large negative magnetoresistance (MR). Although high negative MR has been reported in some magnetic tunnel junctions (MTJs),[2,3] positive MR was found in very few structures so far.[4] In this brief article, we report on our recent progress in the investigation of the novel properties of oxide heterostructures. Firstly, a very unusual positive MR property was found in the heterostructures consisting of a non-magnetic material $SrNb_{0.01}Ti_{0.99}O_3$ (SNTO) and a negative CMR material $La_{0.9}Sr_{0.1}MnO_3$ (LSMO1).[5] Then based on the theory we proposed earlier,[6] a multilayer system with a functional multi-p–n heterojunction consisting of n-type oxygen-deficient $SrTiO_{3-\delta}$ (STO) and p-type LSMO1 on a n-Si substrate was designed and fabricated, in which an electric-field modulation of a large low-field MR (LFMR) up to 80% was realized near room temperature.[7] A deeper theoretical understanding of the transport property in oxide p–n heterojunctions was reached and self-consistent calculations were carried out, from which identical results to the experimental data were obtained.[8,9] Meanwhile, another important characteristic of the picosecond photoelectric effect across the interface in p–n junctions of $La_{0.7}Sr_{0.3}MnO_3$ (LSMO3) on a Si substrate was found,[10] and then a one-order-of-magnitude enhancement of the lateral photovoltage in the structures of both LSMO3/Si and LSMO1/SNTO was observed.[11] This lateral photovoltage can be related to the Dember effect.

[*] Prof. K.-j Jin, Prof. H.-b. Lu, Dr. K. Zhao, C. Ge, M. He, Prof. G.-z. Yang
Beijing National Laboratory for Condensed Matter Physics
Institute of Physics, Chinese Academy of Sciences
Beijing 100190 (China)
E-mail: kjjin@aphy.iphy.ac.cn; hblu@aphy.iphy.ac.cn

DOI: 10.1002/adma.200901046

2. Results

2.1. Fabrication of Oxide Structures and Unusual Positive MR in the Heterostructures of LSMO1/SNTO

A two-dimensional layer-by-layer growth mode, a surface smoothness at the level of a single unit cell, and a very sharp interface are fundamentally important for novel multifunctional properties in perovskite oxide heterostructures and multilayers. In order to fabricate better interfaces in all the structures, computer-controlled laser molecular-beam epitaxy (laser MBE) was applied.[12] In-situ reflection high-energy electron diffraction (RHEED) was used to count the exact number of deposited unit cell layers and control the thickness of the thin film during the growing process. Figure 1a[13] shows the oscillations of RHEED intensity during the growth of a $SrTiO_3$ thin film on a $SrTiO_3$ substrate by laser-MBE, and Figure 1b[13] shows those oscillations for $BaTiO_3/SrTiO_3$ superlattices. The non-decreased high RHEED intensity oscillations indicate that very good two-dimensional growth was maintained in our laser-MBE growing

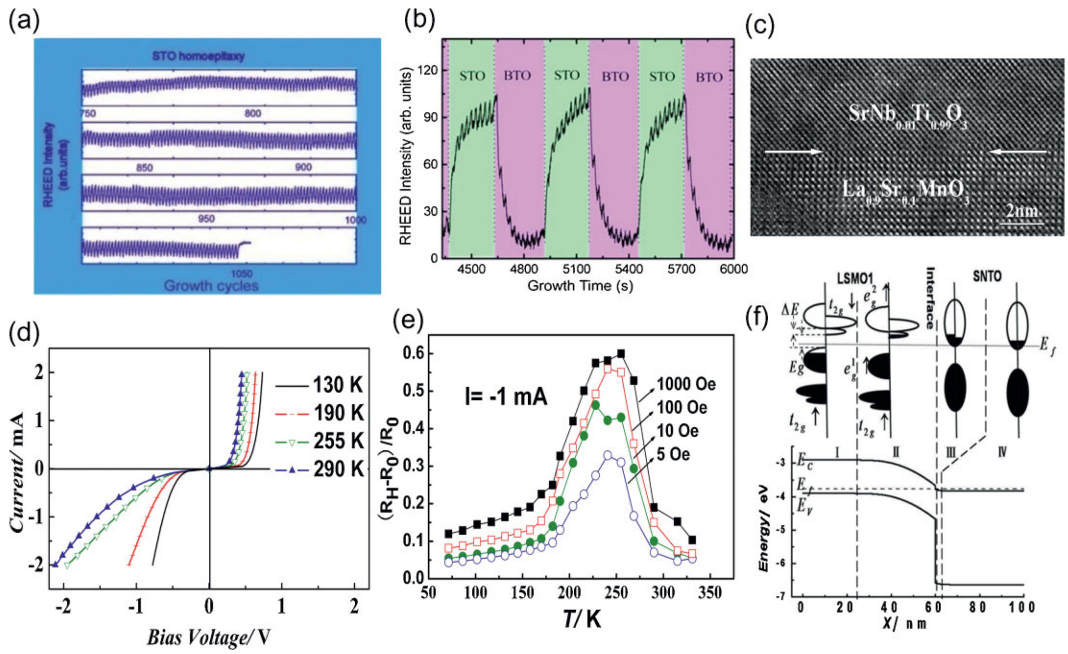

Figure 1. a) A part of RHEED intensity oscillations of $SrTiO_3$ homoepitaxy. b) RHEED intensity oscillations during the epitaxial growth of a $BaTiO_3$ (10 unit cells)/$SrTiO_3$ (10 unit cells) superlattices. c) A cross-sectional HRTEM image of the LSMO1/SNTO interface. d) *I–V* curves of a LSMO1/SNTO p–n junction at different temperatures. e) Temperature dependence of the MR in the heterostructure of LSMO1/SNTO. f) Schematic DOS of the LSMO1/SNTO p–n junction and the calculated band diagram for each region.

process for perovskite oxide structures. With this laser-MBE technique, a p–n junction of LSMO1/SNTO was made by depositing LSMO1 with a thickness of 4000 Å directly on SNTO (001). The X-ray diffraction (XRD) $\theta - 2\theta$ scan curve of the LSMO1/SNTO p–n heterostructure shows only LSMO1 (00*l*) and SNTO (00*l*) peaks, which means that the thin films in the heterostructure are single phases with *c*-axis orientation. The cross-sectional high-resolution transmission electron microscopy (HRTEM) image in Figure 1c[5b] also shows that the interface is perfectly oriented and very sharply defined.

The current versus voltage (*I–V*) characteristics of the LSMO1/SNTO junction without applied magnetic field, measured with a pulse-modulated current source, showing the typical rectifying behavior of a p–n junction are shown in Figure 1d.[6b] Then, a magnetic field perpendicular to the p–n interface was applied. The positive MR behavior of the LSMO1/SNTO p–n junction was measured for a large temperature range under an applied magnetic field varying from 5 to 1000 Oe at a reverse current of 1 mA, and the results are shown in Figure 1e.[6a] The dependence of this positive MR on the bias was also investigated.[6]

It is understandable that certain MTJs have a positive MR property if the tunneling current occurs through two magnetic materials where the charge carriers have anti-parallel spins.[4] However, it is amazing and even seems incredible for a system consisting of a non-magnetic material (SNTO) and a negative CMR material (LSMO1) to exhibit a positive CMR property.

To reveal this mechanism, self-consistent calculations were carried out, and the calculated band structure and schematic density of state of LSMO1/SNTO are plotted in Figure 1f.[6a]

As is shown in Figure 1f, if the reverse bias is large enough, electrons of $e_g\uparrow$ in the valence band in region I can tunnel to the conduction band of $t_{2g}\downarrow$ in region II. With an increasing magnetic field applied to the system, the spin polarizations of the carrier in region I and that in region II are both increased, and so less and less current can be carried from region I to region II because of the scattering between carriers with anti-parallel spins, so that a larger and larger resistance is caused in the system, and a positive MR is created. According to this scenario, the CMR dependence on the bias voltage and temperature can also be explained quantitatively.[6,9]

Based on this understanding, we designed a multilayer structure. As we will present in the following, with such a structure an electric-field modulation of large LFMR near room temperature was realized.[7]

2.2. Electrical Modulation of Magnetoresistance in Multilayer Structures

Electrical modulation of MR in manganite films and heterostructures has attracted a lot of research activities in the hope of finding magnetoelectric coupling at room temperature and being able to explore writing magnetic data with an electric field for data-storage applications.[14] However, obtaining large MR in these structures requires a large magnetic field and low temperature, which does not meet the demand for useful devices operated at low magnetic fields and near room temperature. Recently, electric-field modulation of LFMR up to 80% near room temperature in functional multi-p–n heterojunctions was found,[7] which realized the direct integration of manganite-based memory devices with existing Si-based microelectronic devices.

The STO/LSMO1/STO/LSMO1 heterostructures on n-Si substrates were fabricated by the laser-MBE technique we mentioned above. Usually, $SrTiO_3$ thin films prepared by vacuum processes contain oxygen vacancies and possess some characteristics of n-type semiconductors.[15] Hall-coefficient measurements on our thin films confirmed that the carrier concentrations of the LSMO1 and STO films were 1.19×10^{18} and $-4.83 \times 10^{19}\,\mathrm{cm}^{-3}$, respectively.

The magnetic hysteresis loops of the sample with magnetic field H parallel to the film plane are shown in Figure 2a,[7] which clearly demonstrates that a ferromagnetic phase exists near room temperature in the multi-heterostructure. The current–voltage (I–V) characteristics of the sample over a wide temperature range of 350–80 K are shown in Figure 2b.[7] Figure 2c[7] shows the dependence of the MR of the multi-p–n heterostructure on the reverse bias voltage at $H = 200$ Oe, with H applied parallel to the interface of the heterostructure.

The most interesting phenomenon is the forward bias voltage dependence of the LFMR, in which a crossover of the MR from negative to positive occurs at ca. 0.07 V as shown in Figure 2d.[7] It shows a peak with a maximum of ca. 80% and a dip at ca. 70% for the LFMR at 260 K in a very low magnetic field of 200 Oe occur at about 0.075 and 0.05 V, respectively.

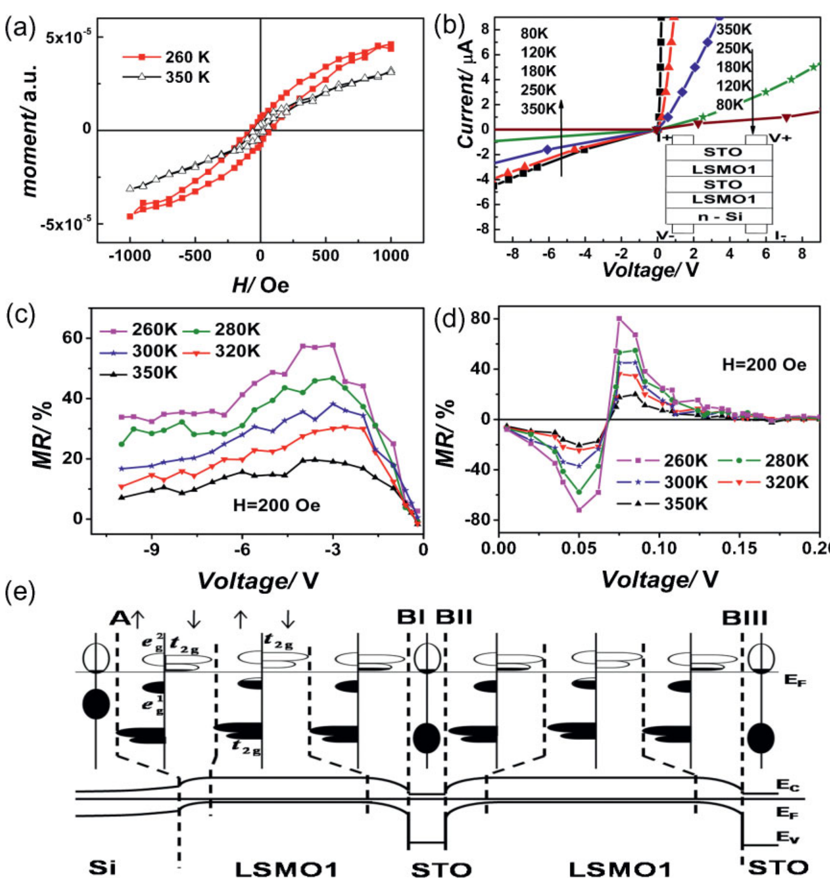

Figure 2. a) Magnetic hysteresis loops for typical STO/LSMO1/STO/LSMO1/Si multi-p–n junctions. b) I–V characteristics of a multi-p–n junction. c) Negative and d) positive bias voltage dependence of the MR, $H = 200$ Oe. e) The schematic electron density of states (DOS) of the multi-p–n junction and the band diagram for each region. A, BI, BII, and BIII denote the four interfaces in the system.

It is well known that the intrinsic MR of the LSMO1 film is small and negative,[16] and STO itself almost has no MR property. So the MR feature and the field-induced spin modulation of the multi-p–n heterojunctions should be unequivocally attributed to the interfacial aspect of the structure.[6,9] The band structure (lower panel) and the density of states for carriers (upper panel) in each region of the system are schematically plotted in Figure 2e.[7] The mechanism of the electrical-field modulated MR reversion (from negative to positive MR) shown in Figure 2d is attributed to the competition of the transport properties at interfaces A, BI, BII, and BIII.[7] We believe that a larger electric modulation of MR should be obtained in the further designing of new structures.

2.3. Enhancement of Lateral Photovoltaic Response in Perovskite Oxide Heterostructures

Another important characteristic of perovskite oxide p–n junctions is the photoelectric effect.[17] Nanosecond and picosecond photoelectric characteristics in LSMO1/SNTO, LSMO3/Si, and STO/Si heterostructures,[10,18a] have been observed, of which the picosecond photovoltage is shown in Figure 3a.[10] However, all these works focused on the photovoltaic effect across the p–n junction of oxides. A lateral photovoltaic (LPV) effect was measured on the surface of one side of the LSMO3/Si heterojunctions.[18b] The general understanding of the LPV for semiconductor p–n junctions is that the optically generated hole–electron pairs cancel out a portion of the barrier space charge resulting in a lateral electric field which induces the lateral flow of majority carriers.[18c] As the majority carriers at the p side are holes and those at the n side are electrons the LPV effect measured between two random positions on the p side and n side should be reversible.

Recently, an unusual transient LPV which was irreversible for both sides of the LSMO1/SNTO p–n junction and for both sides of the LSMO3/Si p–n junction was observed. This phenomenon challenges the well-established theory of LPV mentioned above for conventional semiconductors. A mechanism based on the difference between the mobilities of electrons and holes, that is, the Dember effect,[18d] was introduced to explain this phenomenon. Actually, the Dember effect has come to greater prominence recently as a mechanism for generating THz radiation.[19]

The schematic setup for LPV measurements is shown in the insets of Figure 3. A small area of 0.5 mm in diameter on the p-LSMO1 surface was irradiated by a 308 nm XeCl excimer laser beam (with a pulse width of 20 ns, irradiated energy of 0.15 mJ, and repetition rate of one pulse every five minutes to avoid heating). The maximum LPV values measured on both sides of the heterostructure, $V_{BA}{}^{m}$ and $V_{ED}{}^{m}$ of

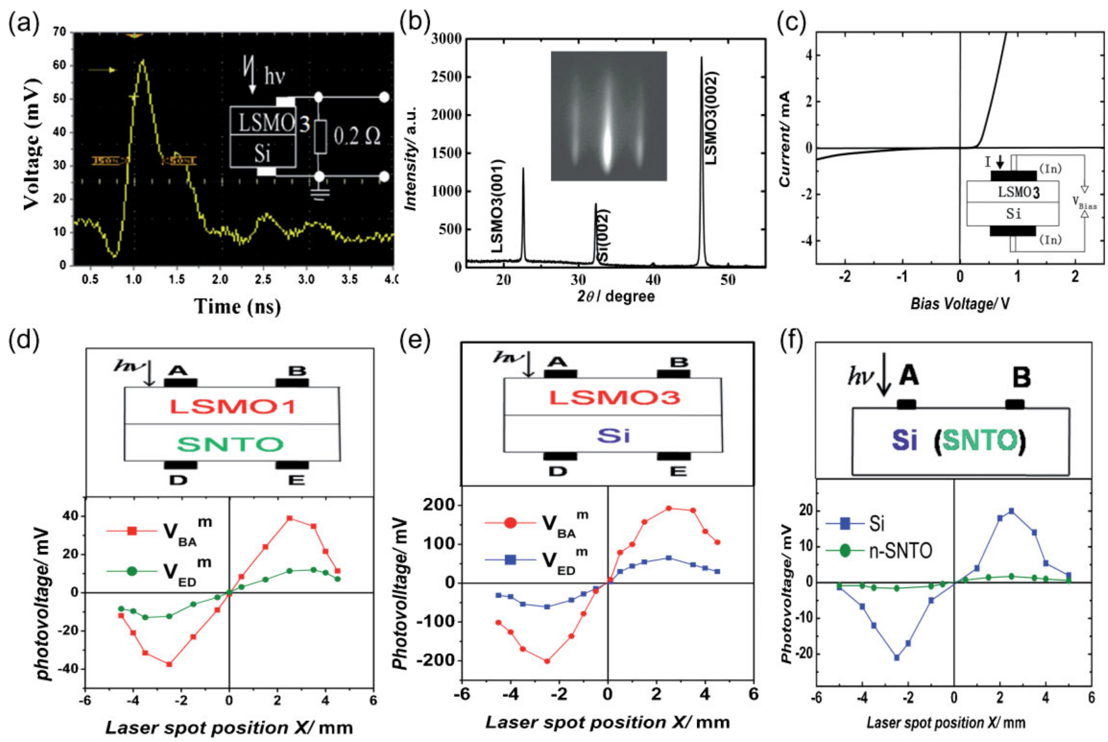

Figure 3. a) The ultrafast photovoltage in the LSMO3/Si p–n junction. b) An XRD pattern of the LSMO3/Si junction. The inset is a RHEED pattern. c) The rectification property of a LSMO3/Si p–n junction. The schematic circuit of a sample measurement is shown in the inset. The peak values of LPV $V_{BA}{}^{m}$ and $V_{ED}{}^{m}$ as a function of the position of the laser spot in the *x*-direction in d) the LSMO1/SNTO and in e) LSMO3/Si heterostructures, the upper panel displays the schematic setup for the LPV measurement. *A* (−3 mm), *B* (3 mm), *D* (−3 mm), and *E* (3 mm) denote the electrodes. f) The peak value of LPV, $V_{BA}{}^{m}$, for n-SNTO (open triangles) and Si (open squares) substrates.

the transient signal are plotted in Figure 3d[11] as a function of the laser spot position (x) on the LSMO1 and SNTO surfaces, respectively. It is clear that the transient LPV depends on the position of the laser spot position and undergoes a sign reversal as the laser spot travels from one electrode to the other. The changeover in sign occurs in the middle ($x = 0$) of the two electrodes. This phenomenon can be explained as follows:

As both electrons and holes are induced by photons and exist on two sides of an oxide p–n junction, the diffusion mobility difference of electrons and holes from the laser spot point causes the same sign (positive or negative) of LPV on both sides of the p–n junction. The smaller amount of induced carriers on the n-SNTO side compared to that on the p-LSMO1 side causes a reduction in the measured LPV on the n-SNTO surface compared to that of the p-LSMO1 surface. It should be noted that only strong light can make the Dember effect LPV large enough to be observed. The photon energy at 308 nm (ca. 4.03eV) is higher than the bandgap of LSMO1 (ca. 1.0 eV) and SNTO (ca. 3.2 eV), so that electron–hole pairs can be generated in both the p-LSMO1 layer and the n-SNTO substrate. Note that the carried out absorption measurements have proved that the laser can go through the LSMO1 thin film with a slight decay in amplitude.

Similar measurements were taken in the LSMO3/Si heterostructures fabricated by laser-MBE.[11] LSMO3/Si is also a p–n heterojunction whose structure and transport properties have been widely studied.[10,18a] The rectification property is shown in Figure 3c.[11] The crystallization of the LSMO3 film was examined in situ by RHEED, and was also characterized ex situ using XRD analysis. The RHEED pattern of a 400-nm thick LSMO3 film is shown in the inset of Figure 3b.[10] The LPV results are shown in Figure 3e.[11] Comparing Figure 3d and 3e, we can see that a much larger LPV, induced by the Dember effect, occurs in LSMO3/Si p–n junctions than in LSMO1/SNTO p–n junctions. The reason for this may be that the photoelectrons gain more kinetic energy in LSMO3/Si junctions than in LSMO1/SNTO junctions, as the bandgap of Si (ca.1.1 eV) is much narrower than that of SNTO (ca. 3.2 eV).

To compare the LPV in the heterostructures and that in simple oxides or semiconductors, the LPV measurements for n-SNTO and n-Si substrates were also carried out and the results are shown in Figure 3f.[11] From this figure, we can see that the LPV in n-Si is much larger than that in n-SNTO, which further confirms the above explanation for the Dember-effect-induced LPV in the heterostructures of LSMO3/Si and LSMO1/SNTO.

Comparing the results of LPV in heterojunctions shown in Figures 3d and 3e, and those in simple substrates shown in Figure 3f, we can find that an LPV effect that is one order of magnitude larger is produced in heterostructures than in plain samples (SNTO or Si). One of the reasons for this may be the higher amount of charge carriers in the interface region because of a transfer of electrons from the p-side to the n-side.[20]

RESEARCH NEWS

3. Conclusions and Perspectives

Based on the understanding of the mechanisms behind the unusual positive MR occurring in perovskite p–n heterostructures, multi-p–n heterostructures have been artificially designed, in which quite large electrical modulation of the MR is obtained. These results have clearly demonstrated that the interface effect in oxide heterostructures or interface competition effect in multi-heterostructures allows the generation of novel magneto-transport phenomena. It is expected that further studies on the design of new structures can help to obtain larger electric modulations of the magnetoresistance.

Moreover, quite large Dember-effect-induced LPVs have been observed in LSMO1/SNTO and LSMO3/Si p–n heterostructures. LPV effects that are ten times larger are produced in heterostructures compared to that of the substrates (plain samples), which strongly suggests many potential applications of the greatly enhanced Dember effect in heterostructures, such as photoelectric detectors or even new sources of terahertz radiation.

Acknowledgements

The authors acknowledge the financial support from the National Natural Science Foundation of China and the National Basic Research Program of China.

Published online: August 12, 2009

[1] a) *Science* **2007**, *318*, 1844. b) A. Ohtomo, H. Y. Hwang, *Nature* **2004**, *427*, 423. c) E. Dagotto, *Science* **2007**, *318*, 1076.

[2] a) C. Mitra, G. Kobernik, K. Dorr, K. H. Muller, L. Schultz, P. Raychaudhuri, R. Pinto, E. Wieser, *J. Appl. Phys.* **2002**, *91*, 7715. b) T. Obata, T. Manako, Y. Shimakawa, Y. Kubo, *Appl. Phys. Lett.* **1999**, *74*, 290.

[3] J. Z. Sun, D. W. Abraham, K. Roche, S. S. P. Parkin, *Appl. Phys. Lett.* **1998**, *73*, 1008.

[4] C. Mitra, P. Raychaudhuri, K. Dorr, K. H. Muller, L. Schultz, P. M. Oppeneer, S. Wirth, *Phys. Rev. Lett.* **2003**, *90*, 017202.

[5] a) H. B. Lu, G. Z. Yang, Z. H. Chen, S. Y. Dai, Y. L. Zhou, K.-j. Jin, B. L. Cheng, M. He, L. F. Liu, Y. Y. Fei, W. F. Xiang, L. Yan, *Appl. Phys. Lett.* **2004**, *84*, 5007. b) H. B. Lu, S. Y. Dai, Z. H. Chen, Y. L. Zhou, B. L. Cheng, K.-j. Jin, L. F. Liu, G. Z. Yang, X. L. Ma, *Appl. Phys. Lett.* **2005**, *86*, 032502.

[6] a) K.-j. Jin, H. B. Lu, Q. L. Zhou, K. Zhao, B. L. Cheng, Z. H. Chen, Y. L. Zhou, G. Z. Yang, *Phys. Rev. B* **2005**, *71*, 184428. b) K.-j. Jin, H. B. Lu, Q. L. Zhou, K. Zhao, G. Z. Yang, *J. Magn. Magn. Mater.* **2006**, *303*, 329.

[7] K. Zhao, K.-j. Jin, H. B. Lu, M. He, Y. H. Huang, G. Z. Yang, J. D. Zhang, *Appl. Phys. Lett.* **2008**, *93*, 252110.

[8] a) P. Han, K.-j. Jin, H. B. Lu, Q. L. Zhou, Y. L. Zhou, G. Z. Yang, *Appl. Phys. Lett.* **2007**, *91*, 182102. b) C. L. Hu, P. Han, K.-j. Jin, H. B. Lu, G. Z. Yang, *J. Appl. Phys.* **2008**, *103*, 053701. c) J. Qiu, K.-j. Jin, P. Han, H. B. Lu, C. L. Hu, B. P. Wang, G. Z. Yang, *Europhys. Lett.* **2007**, *79*, 57004.

[9] a) C. L. Hu, K.-j. Jin, P. Han, H. B. Lu, L. Liao, G. Z. Yang, *Appl. Phys. Lett.* **2008**, *93*, 162106. b) C. L. Hu, K.-j. Jin, P. Han, H. B. Lu, L. Liao, G. Z. Yang, *Solid State Commun.* **2009**, *149*, 334.

[10] H. B. Lu, K.-j. Jin, Y. H. Huang, M. He, K. Zhao, B. L. Cheng, Z. H. Chen, Y. L. Zhou, S. Y. Dai, G. Z. Yang, *Appl. Phys. Lett.* **2005**, *86*, 241915.

[11] K.-j. Jin, K. Zhao, H. B. Lu, L. Liao, G. Z. Yang, *Appl. Phys. Lett.* **2007**, *91*, 081906.

[12] G. Z. Yang, H. B. Lu, Z. H. Chen, D. F. Cui, H. S. Wang, H. Q. Yang, F. Y. Miao, Y. L. Zhou, L. Li, *Sci. China, Ser. A: Math, Phys, Astron. & Technol. Sci.* **1998**, *28*, 260.

[13] G. Z. Yang, H. B. Lu, F. Chen, T. Zhao, Z. H. Chen, *J. Cryst. Growth* **2001**, *227*, 929.

[14] a) S. B. Ogale, V. Talyansky, C. H. Chen, R. Ramesh, R. L. Greene, T. Venkatesan, *Phys. Rev. Lett.* **1996**, *77*, 1159. b) M. Tokunaga, H. Song, Y. Tokunaga, T. Tamegai, *Phys. Rev. Lett.* **2005**, *94*, 157203. c) A. Asamitsu, Y. Tomioka, H. Kuwahara, Y. Tokura, *Nature* **1997**, *388*, 50.

[15] O. N. Tufte, P. W. Chapman, *Phys. Rev.* **1967**, *155*, 796.

[16] H. Kawano, R. Kajimoto, M. Kubota, H. Yoshizawa, *Phys. Rev. B* **1996**, *53*, R14709.

[17] a) T. Muramatsu, Y. Muraoka, Z. Hiroi, *Solid State Commun.* **2004**, *132*, 351. b) J. R. Sun, C. H. Lai, H. K. Wong, *Appl. Phys. Lett.* **2004**, *85*, 37.

[18] a) Y. H. Huang, M. He, K. Zhao, H. F. Tian, H. B. Lu, K.-j. Jin, Z. H. Chen, Y. L. Zhou, J. Q. Li, G. Z. Yang, *Chin. Phys. Lett.* **2005**, *22*, 2950. b) K. Zhao, K.-j. Jin, H. B. Lu, Y. H. Huang, Q. L. Zhou, M. He, Z. H. Chen, Y. L. Zhou, G. Z. Yang, *Appl. Phys. Lett.* **2006**, *88*, 141914. c) S. Amari, *J. Phys. III France* **1991**, *1*, 1669. d) J. I. Pankove, *Optical Processes in Semiconductors*, Prentice-Hall Inc, Englewood Cliffs, NJ **1971**.

[19] R. Kersting, K. Unterrainer, G. Strasser, H. F. Kauffmann, E. Gornik, *Phys. Rev. Lett.* **1997**, *79*, 3038.

[20] H. K. Yadav, K. Sreenivas, V. Gupta, *Appl. Phys. Lett.* **2007**, *90*, 172113.